

## An ultra-efficient energy transfer beyond plasmonic light scattering

Sze-Ming Fu, Yan-Kai Zhong, and Albert Lin

Citation: *Journal of Applied Physics* **116**, 183103 (2014); doi: 10.1063/1.4901325

View online: <http://dx.doi.org/10.1063/1.4901325>

View Table of Contents: <http://scitation.aip.org/content/aip/journal/jap/116/18?ver=pdfcov>

Published by the [AIP Publishing](#)

---

### Articles you may be interested in

[Directional plasmonic scattering from metal nanoparticles in thin-film environments](#)

*Appl. Phys. Lett.* **104**, 081110 (2014); 10.1063/1.4866669

[Multiple-scattering formalism beyond the quasistatic approximation: Analyzing resonances in plasmonic chains](#)

*AIP Conf. Proc.* **1475**, 158 (2012); 10.1063/1.4750128

[Tuning the wavelength drift between resonance light absorption and scattering of plasmonic nanoparticle](#)

*Appl. Phys. Lett.* **99**, 101901 (2011); 10.1063/1.3636403

[Scattering suppression in plasmonic optics using a simple two-layer dielectric structure](#)

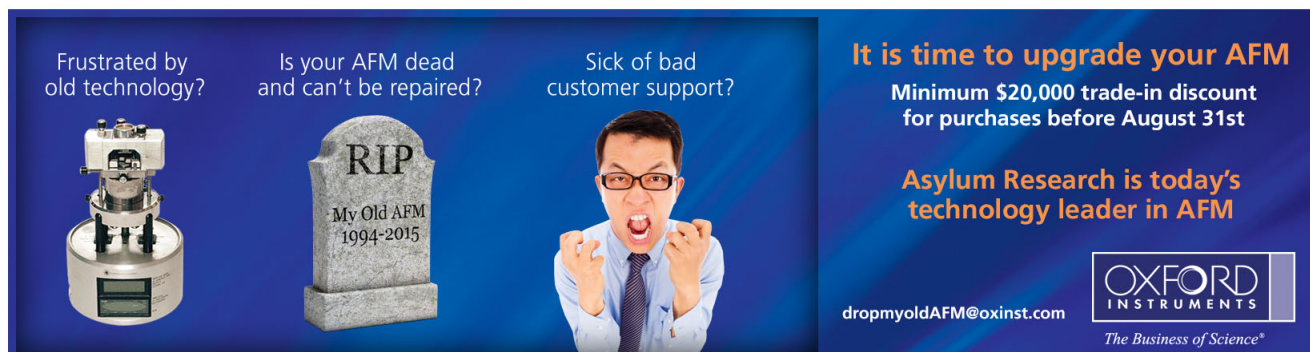
*Appl. Phys. Lett.* **98**, 221108 (2011); 10.1063/1.3597620

[Distance-controlled scattering in a plasmonic trap](#)

*Appl. Phys. Lett.* **96**, 073104 (2010); 10.1063/1.3291564

---

Frustrated by old technology?      Is your AFM dead and can't be repaired?      Sick of bad customer support?



**It is time to upgrade your AFM**  
Minimum \$20,000 trade-in discount for purchases before August 31st

**Asylum Research is today's technology leader in AFM**

[dropmyoldAFM@oxinst.com](mailto:dropmyoldAFM@oxinst.com)

**OXFORD INSTRUMENTS**  
The Business of Science®

# An ultra-efficient energy transfer beyond plasmonic light scattering

Sze-Ming Fu, Yan-Kai Zhong, and Albert Lin<sup>a)</sup>

*Department of Electronic Engineering, National Chiao-Tung University, Hsinchu 30010, Taiwan*

(Received 20 September 2014; accepted 29 October 2014; published online 11 November 2014)

The energy transfer between nano-particles is of great importance for, solar cells, light-emitting diodes, nano-particle waveguides, and other photonic devices. This study shows through novel design and algorithm optimization, the energy transfer efficiency between plasmonic and dielectric nano-particles can be greatly improved. Using versatile designs including core-shell wrapping, supercells and dielectric mediated plasmonic scattering,  $0.05 \text{ dB}/\mu\text{m}$  attenuation can be achieved, which is 20-fold reduction over the baseline plasmonic nano-particle chain, and 8-fold reduction over the baseline dielectric nano-particle chain. In addition, it is also found that the dielectric nano-particle chains can actually be more efficient than the plasmonic ones, at their respective optimized geometry. The underlying physics is that although plasmonic nano-particles provide stronger coupling and field emission, the effect of plasmonic absorption loss is actually more dominant resulting in high attenuation. Finally, the group velocity for all design schemes proposed in this work is shown to be maintained above  $0.4c$ , and it is found that the geometry optimization for transmission also boosts the group velocity. © 2014 AIP Publishing LLC. [<http://dx.doi.org/10.1063/1.4901325>]

## I. INTRODUCTION

Research in plasmonics is attracting a considerable interest<sup>1–6</sup> since it allows to engineer innovative photonic and optoelectronic devices. Among various novel plasmonic applications, the energy transfer between plasmonic nano-particles (NPs) is a peculiar phenomenon that has been found since 2003.<sup>7–9</sup> The fact that the coupling of the optical field can be tailored below the diffraction limit makes it very promising for various photonic applications.<sup>9,10</sup> Recently, dielectric nano-particles are also shown to be capable of initiate energy transfer through Mie scattering,<sup>11</sup> but it is generally believed in these studies,<sup>11</sup> dielectric nano-particle chains are less efficient than metallic ones due to the lack of plasmonic field emission. In this work, it is going to show that through proper design and optimization, dielectric nano-particle chains can be even more efficient than metallic ones. This observation is not surprising, if the literature for solar cell optics<sup>12–14</sup> is reviewed. In these works, it has been found that the enhancement of the photovoltaic effect for plasmonic and dielectric nano-particles is of the same amount. In addition, if the nano-particles are placed at the front side of solar cells, dielectric nano-particles are actually far more efficient. As long as the energy transfer efficiency can be improved for plasmonic and dielectric nano-particles, the application to solar cells, photodectors, photonic crystals, and nano-particles waveguides (NPWG) will become more practical. Since NPWG is the most relevant photonic application for NP chains, in this study, it is used as an example to show the effect of various novel designs. Once the energy transfer efficiency in NPWG can be improved, the proposed design strategies can easily be applied to other photonic applications using NPs.

Two issues remain for NPWG. One is the choice of dielectric or metallic nano-particles. While metallic NP initiates surface plasmons (SPs), it also suffers from SP absorption. On the other hand, dielectric NPs does not suffer from severe absorption, but the lack of SP emission may make the design more complicated. Another issue for NPWG is the high attenuation loss for NP chains. Unlike conventional metallic slab or dielectric slab waveguides where the optical wave is well-confined in the guiding structure, the waveguiding of NPWG generally counts on the Mie mode coupling between NPs in free space. This results in very high attenuation factors. In order to reduce this attenuation loss and improve the practicability of NP chains for photonic devices, versatile design schemes and geometry optimization is inevitable. In this works, several new design schemes are employed to improve the energy transfer efficiency for NP chains, and pronounced results are observed.

## II. PROBLEM SET-UP AND ENHANCED ENERGY TRANSFER FOR NANO-PARTICLE CHAINS

The basic structure of SP and dielectric NP chains are first investigated where NPs are placed in a straight line. Their attenuation factors are calculated as the baseline for the comparison afterward. The spacing and the sphere diameter are adjusted by genetic algorithm to maximize the energy transfer efficiency. Aperiodicity is also included in the study, to explore the possibility of aperiodic NP chain for waveguiding.

The second structure is the core-shelled structure. The core-shelled design can be incorporated into both plasmonic and dielectric NPWGs. The advantage of core-shelled structure for SP NPs is the better trade-off between scattering and absorption cross sections, compared to the unwrapped basic metallic NP chains. The trade-off is due to the fact that the dielectric wrapping can generally decrease the plasmonic

<sup>a)</sup>email: [dtd5746@gmail.com](mailto:dtd5746@gmail.com)

absorption. Care should be taken since the decrease of SP absorption can also lead to decreased SP emission. For dielectric NP chains, the core-shelled design consists of inner dielectric core and outer dielectric wrapping. It is found in this work that the advantage of core-shelled structure also exists for purely dielectric NP chains due to adiabatic coupling between core-shelled dielectric NPs.

The third versatile design is through the concept of super-cells to further increase the design flexibility. Supercell design has been proved to be effective in photonic crystals such as photonic defect modes or coupled cavity waveguides (CCW) and coupled resonator optical waveguide (CROW).<sup>15,16</sup> The arrangement of the NPs in supercell is the key to increasing the transmittance through the NP chain.

The fourth structure under study is dielectric-mediated surface plasmonic energy transfer where the interlaced placement of dielectric and plasmonic NPs is proposed. The mixture of dielectric and plasmonic Mie scattering is turned out to be very efficient for NPWG application. The hybrid design is actually a very promising route for plasmonic photonics. This is due to the fact that plasmonic NPs normally provide stronger field emission while dielectric NPs can provide zero absorption loss. The well-optimized hybrid design can utilize the advantages of both dielectric and SP nano-particles while minimizing the adverse effects. The advantage over the second design, i.e., dielectric wrapped plasmonic NPs, is the simpler fabrication for interlaced hybrid design.

Genetic algorithm is chosen as a global optimization algorithm due to its success in different fields of science and engineering,<sup>17–20</sup> and the advantage that it does not require initial guesses. The material parameters are from Rsoft material database<sup>21</sup> and the refractive index for dielectric NPs is  $n_r = 3.5$  unless otherwise specified. The calculation method is based on eigen mode propagation (EMP) implemented by Rsoft ModeProp. The polarization is p-polarization in two-dimensional (2D) simulation domain to study the effect surface plasmon. Generalization to three-dimensional NPWG is trivial based on the study and design scheme presented here. The 2D design, however, has the advantage of simpler semiconductor processing and simpler integration into optoelectronic integrated circuits (OEIC). The choice of waveguide operation wavelength is  $1 \mu\text{m}$ . For dielectric NP chain, the selection of wavelength is un-important due to the geometry scalability of dielectric NP design for different target wavelengths. For plasmonic NP chains, the selection of wavelength should be within the plasmonic emission wavelength of a specific metallic material. The scalability of plasmonic waveguide using the same material is more difficult since the metallic dielectric response is generally not a constant for different wavelength ranges. For different wavelength application, different plasmonic materials have to be used for NPWGs. Silver nano-particles have been known to be capable of the surface plasmon emission over the visible and near infrared range<sup>22–24</sup> so  $1 \mu\text{m}$  is chosen here for SP NPWG. The visible wavelength  $\lambda = 560 \text{ nm}$  is also conducted for basic SP nano-particle chain, similar to.<sup>7–9</sup> The energy transfer after geometry optimization is slightly less efficient than  $\lambda = 1000 \text{ nm}$ .

### III. BASELINE DESIGN FOR PLASMONIC AND DIELECTRIC NANO-PARTICLE CHAINS

It is illustrative to examine the basic design of nano-particle chains for plasmonic and dielectric energy transfer. The schematics are illustrated in Fig. 1. The sphere diameter and the spacing are the key parameters since this affects the Mie mode excited and the mode coupling efficiency between NPs. In Fig. 1, aperiodicity is also possible where the spacing between each nano-particle is adjusted individually to maximize the energy transfer efficiency through the NPWG. Nonetheless, based on our study, the aperiodic design does not have a significant impact on the transmittance for NPWG. The physical reason is that the waveguiding is, in fact, a periodic phenomenon, and therefore introducing aperiodicity does not have much physical meaning as far as waveguiding is concerned. The optimized geometry for basic periodic NP chain is  $d_s = 210 \text{ nm}$ ,  $D = 201 \text{ nm}$  for plasmonic NP chain and  $d_s = 194 \text{ nm}$ ,  $D = 194 \text{ nm}$  for dielectric NP chain. Silver is used for plasmonic NPs, and  $n_r = 3.5$  is assumed for dielectric NPs. The attenuation factor is  $0.95 \text{ dB}/\mu\text{m}$  for plasmonic NPWG and is  $0.45 \text{ dB}/\mu\text{m}$  for dielectric NPWG. Compared to the literature,<sup>11,25</sup> the attenuation factors are around the same order. The attenuation of NPWG is generally higher compared to other waveguide structures including photonic crystal waveguide,<sup>15,26,27</sup> coupled photonic crystal cavity waveguides,<sup>15,16</sup> conventional index-guided waveguide,<sup>15,26,27</sup> metallic waveguides,<sup>28</sup> and etc. This is due to fact that the confinement by solely NPs in free space is not sufficient for efficient waveguiding. Nonetheless, advantage associated with NPWG is that simpler and smaller geometry. This is especially obvious when NPWG is compared to photonic crystal based devices such as photonic crystal waveguides<sup>15,26,27</sup> or photonic crystal coupled-cavity waveguides<sup>15,16</sup> where an entire arrays of nano-particles is necessary. From the thorough geometry optimization in this study for both plasmonic and dielectric NPWGs, it is observed that the dielectric one can provide

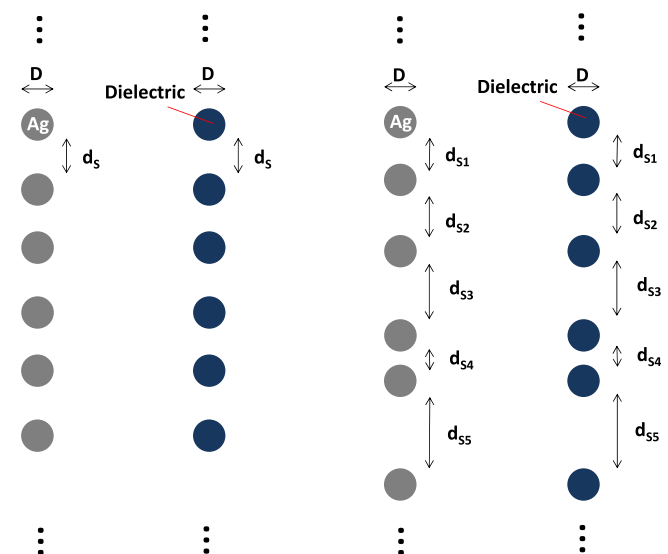


FIG. 1. Illustration of the basic NP chain for plasmonic NPs and dielectric NPs and the geometrical parameters to be optimized. Aperiodicity is also possible to be incorporated into NPWG design.

lower attenuations, due to the absence of plasmonic absorption. Fig. 2 shows the field profile plots for continuous wave (CW) energy transfer at design wavelength ( $1 \mu\text{m}$ ).

#### IV. CORE-SHELLED STRUCTURES: DIELECTRIC-WRAPPED PLASMONICS AND ADIABATIC MODE COUPLING

In Fig. 3, the core-shelled design is introduced to further decrease the attenuation factor for nano-particle chains. For the plasmonic design, the wrapping of the metallic NPs by a dielectric spacer can generally decrease the surface plasmon absorption loss. For the dielectric design, the core-shelled design incorporates two dielectric materials whose refractive index is different and adjusted independently during optimization. The thickness of the dielectric wrapping for the plasmonic NP chain should be adjusted carefully in order to achieve the maximal energy transfer where the balance between plasmonic absorption and emission is achieved. For the dielectric NP chain, the improvement in energy transfer efficiency is due to the adiabatic mode coupling where the refractive-index-change becomes less abrupt and therefore attain low attenuation.

The optimized geometry for core-shelled NP chain is  $d_s = 298 \text{ nm}$ ,  $D = 300 \text{ nm}$ ,  $\delta = 270 \text{ nm}$  for the plasmonic NP chain. The optimized geometry  $d_s = 285 \text{ nm}$ ,  $D = 300 \text{ nm}$ ,  $\delta = 126 \text{ nm}$  for the dielectric NP chain, and the optimized refractive index is 1.85 for the outer dielectric material (wrapping) and 2.83 for the inner dielectric material (core). Since in optimization, the freely adjusted index for core and wrapping dielectric does not guarantee the index is high to low from core to wrapping, the optimized result, i.e., higher index for core and lower index for wrapping, reveals the adiabatic mode coupling is the most efficient way for dielectric NPWG. The gradual change of refractive index is the key to achieving better coupling between adjacent dielectric NPs. This is similar to adiabatic coupling in graded index anti-reflection coating for solar cells. The attenuation factor is  $0.24 \text{ dB}/\mu\text{m}$  for plasmonic NPWG and is  $0.21 \text{ dB}/\mu\text{m}$  for dielectric NPWG. The improvement in attenuation factor is about 4-fold reduction for plasmonic design, and about 2-

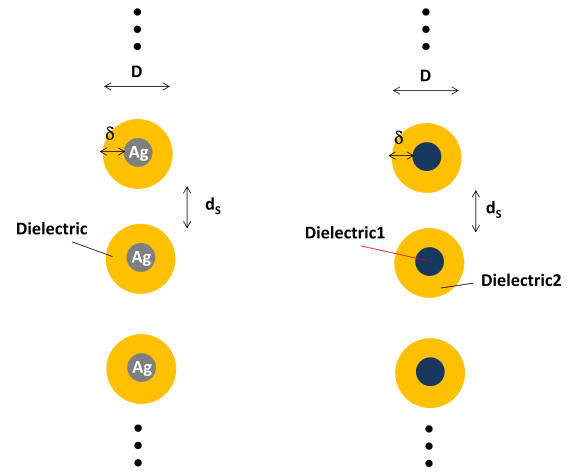


FIG. 3. Illustration of core-shelled design. (Left) Plasmonic NPWG and the geometrical parameters to be optimized. The silver sphere is wrapped by a dielectric material. (Right) The adiabatic dielectric NPWG design.

fold reduction for dielectric design, compared to the baseline design in Sec. III. Fig. 4 shows the field profile plots for CW energy transfer at design wavelength ( $1 \mu\text{m}$ ).

#### V. SUPER-CELL DESIGN FOR DIELECTRIC NANO-PARTICLE WAVEGUIDES

In Fig. 5, the supercell design is incorporated into dielectric NP chains to further increase the energy transfer efficiency. The idea of supercell is conceptually similar to multi-atomic molecules where more than one atom exists in a molecule. The mathematical reason why the energy transfer in NP chains can be more efficient with the supercell design is that more design variable and flexibility is available, achieving larger searching space in genetic algorithm optimization. The geometry parameters to be adjusted include the nano-particle diameters in a supercell, the vertical and horizontal spacing between the NPs in a supercell, and the spacing between each supercell. Intuitively, the adjustment of  $d_v$  seems to control the vertical energy coupling between NP3 and NP4, and the adjustment of  $d_H$  seems to controls the horizontal coupling between NP1 and NP2. In fact, from the calculation and optimization, it can be seen that most efficient

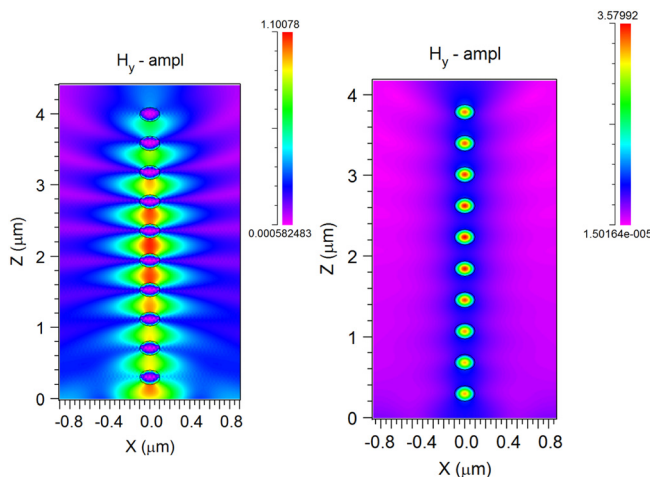


FIG. 2. The  $H_y$  field for basic (left) plasmonic nano-particle waveguides and (right) dielectric nano-particle waveguides.

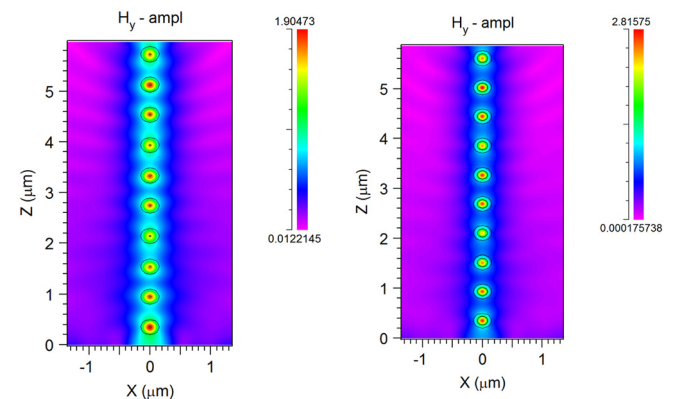


FIG. 4. The  $H_y$  field for basic (left) plasmonic nano-particle waveguide with core-shell design and (right) dielectric nano-particle waveguide with core-shell design.

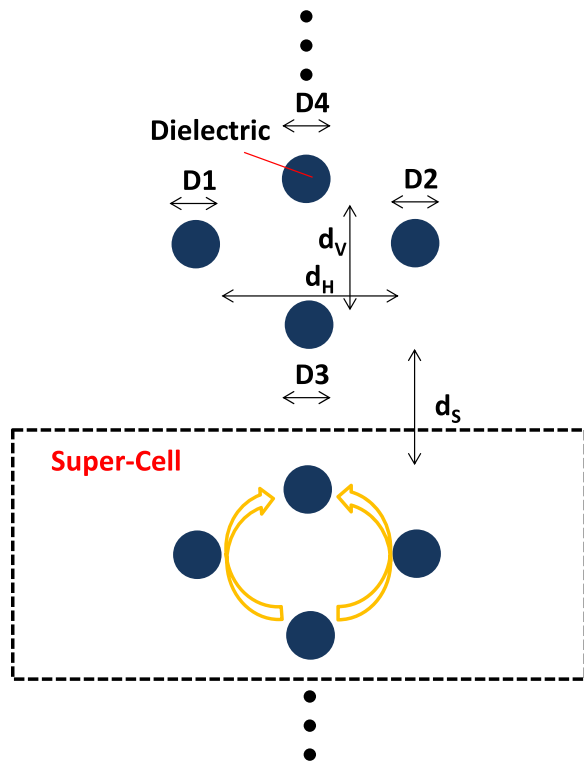


FIG. 5. Illustration of dielectric NPWG with super cell design and the geometrical parameters to be optimized by genetic algorithm.

mode coupling is through the path NP4 to NP1/NP2 to NP3. As a result, the purpose of adjusting  $d_V$  and  $d_H$  in a unit cell is to maximize the energy transfer efficiency through this two-step process. Physically, the intermediate scattering sites, i.e., dielectric nano-particles NP1 and NP2 strengthen the coupling between NP3 and NP4, compared to the baseline case where only direct vertical coupling between NP3 and NP4 is possible. This is illustrated by the arrows in Fig. 5 and evident from the field plot for  $E_x$  in Fig. 6(b). The optimized geometry for supercell design for dielectric NP chain is  $D1 = 183$  nm,  $D2 = 185$  nm,  $D3 = 190$  nm,  $D4 = 190$  nm,  $H = 298$  nm,  $V = 265$  nm, and  $d_S = 200$  nm. The attenuation factor is  $0.05$  dB/ $\mu\text{m}$ . The improvement in attenuation factor

is 8-fold reduction, compared to the baseline dielectric design in Sec. III. Fig. 6 shows the field plots for CW energy transfer for the design wavelength ( $1\ \mu\text{m}$ ) and for higher order propagation modes ( $0.5\ \mu\text{m}$ ). The higher order mode nature is evident from observing the field profile within the dielectric NP where two anti-nodes exist.

## VI. DIELECTRIC-MEDIATED PLASMONIC SCATTERING FOR PLASMONIC NANO-PARTICLE WAVEGUIDES

Fig. 7 shows the design of a hybrid plasmonic-dielectric NP chain. The concept of supercell is also incorporated into this hybrid design. Plasmonic design of all kinds inevitably suffers from the problem of plasmon absorption loss. Dielectric wrapping as presented in Sec. IV is one way to mitigate this problem. Another more versatile design is using a hybrid plasmonic-dielectric Mie mode scattering where the dielectric and plasmonic NPs are interlaced to initiate energy transfer. The interlaced hybrid scheme has the advantage of simpler fabrication over the dielectric wrapped plasmonic NPs in Sec. IV. The schematics and geometrical parameters to be optimized are also illustrated in Fig. 7. This includes the diameters of the dielectric and metallic nano-particles, the vertical ( $d_V$ ) and horizontal spacing ( $d_H$ ) within a unit cell, and the spacing between each unit cell ( $d_S$ ). The dielectric nano-particles NP1 and NP2 can aid the energy transfer by providing intermediate light scattering sites. This is illustrated by the arrows in Fig. 7 and evident from the field profile plots in Fig. 8(b). In order to fully utilize these intermediate sites, the geometry has to be carefully optimized where genetic algorithm is very useful. Physically, the hybrid plasmonic and non-plasmonic Mie scattering can initiate energy transfer in NP chains with less plasmonic absorption. This is easy to conceive since the number of metallic nano-particles is reduced by inserting dielectric nano-particles into the design. Ideally, the hybrid design may provide the most efficient energy transfer by possessing the advantage of both dielectric and metallic nano-particles, i.e., low absorption for dielectric NPs and strong plasmonic field emission for metallic NPs. Nonetheless, compared to the

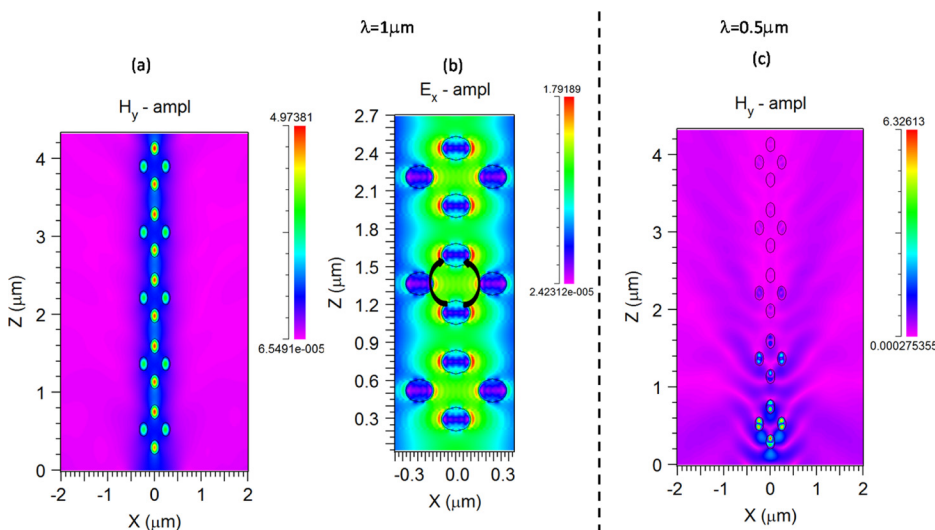


FIG. 6. The field profiles for the dielectric NPWG with supercell design (a)  $H_y$  field at design wavelength  $\lambda = 1\ \mu\text{m}$  (b)  $E_x$  field at design wavelength  $\lambda = 1\ \mu\text{m}$  (c)  $H_y$  field at higher order propagation modes  $\lambda = 0.5\ \mu\text{m}$ .

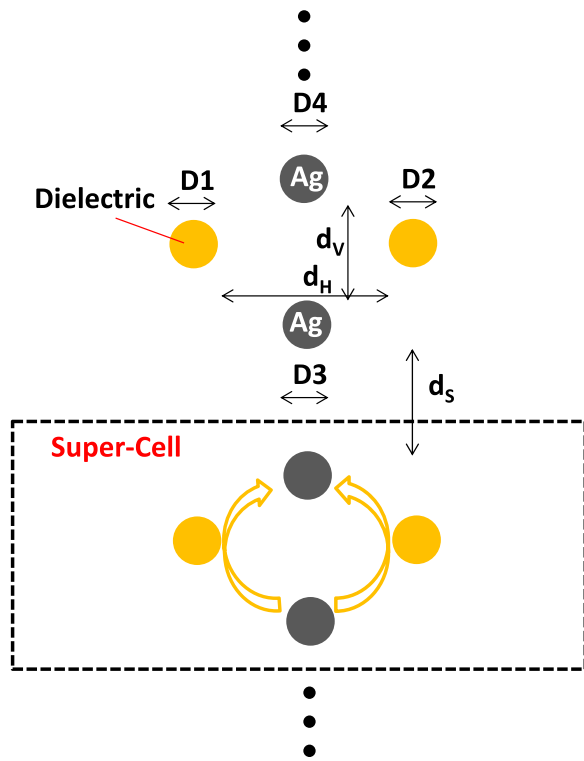


FIG. 7. Illustration of plasmonic NPWG with interlaced dielectric and plasmonic nano-particles and the geometrical parameters to be optimized by genetic algorithm.

optimized result in Sec. V, the hybrid design here does not provide a comparably low attenuation factor. This observation is consistent with what is reported in Sec. III. In Sec. III, it is shown that for the baseline design of NP chains, the dielectric one provides lower attenuation after full geometrical optimization. The optimized geometry for the dielectric-mediated plasmonic NP chain in this section is  $D1 = 161$  nm,  $D2 = 136$  nm,  $D3 = 172$  nm,  $D4 = 141$  nm,  $H = 300$  nm,  $V = 150$  nm,  $d_S = 276$  nm, and the optimized refractive index for the interlaced dielectric NPs is 2.06. The attenuation factor is  $0.25\text{db}/\mu\text{m}$ . The improvement in attenuation factor is 4-fold reduction, compared to the baseline plasmonic design in Sec. III. Fig. 8 shows the field plots for CW energy

transfer for the design wavelength ( $1\ \mu\text{m}$ ) and below cutoff ( $2\ \mu\text{m}$ ). From the field plot in Fig. 8, the emitted photon from plasmonic NP3 is coupled to dielectric NP1 and NP2, and then the forward diffracted photons from dielectric NP1 and NP2 is coupled to plasmonic NP4.

## VII. PULSED EXCITATION AND WAVEGUIDE GROUP VELOCITY

Table I shows the group velocity of different nano-particle chains. The calculation of group velocity is by pulse excitation using finite different time domain (FDTD) method as illustrated in Fig. 9. Waveguide group velocity is of particular important for passive photonic or active optoelectronic application. This is due to the fact that the group velocity determines the energy flow velocity while the phase velocity in general has less physical meaning. From Table I, the group velocity can be maintained above  $0.4c$ , close to the highest value reported in literature.<sup>8</sup> The high group velocity here is not a coincidence, and it is the result of the optimization with respect to the attenuation factor or transmittance. For the case of plasmonic nano-particles, it is not very difficult to conceive the idea that the optimization of group velocity and transmittance is actually quite the same thing. This is due to the fact that if the light pulse can move through the NP chain faster, the absorption in SP NPs can be significantly reduced. On the contrary, if the group velocity is slow, the absorption will be significant, similar to the case of the slow-light enhancement for solar cell light trapping. In the case of purely dielectric design, if the light pulse can move faster, the escaping power into the lateral direction, i.e., beam divergence, will be minimized. As a result, the optimization of transmittance and group velocity is still along the same line.

Fig. 10 shows the spectral responses for various NPWGs in this paper. Since the optimized propagation modes in this study are fundamental modes for various designs, at shorter wavelength below  $1\ \mu\text{m}$ , higher order mode will in general be excited along the NP chains. Nonetheless, the higher order modes of NPWG for a specific geometry, is generally not of decent waveguiding. This is due to the geometry is optimized for the fundamental modes. This is evident from

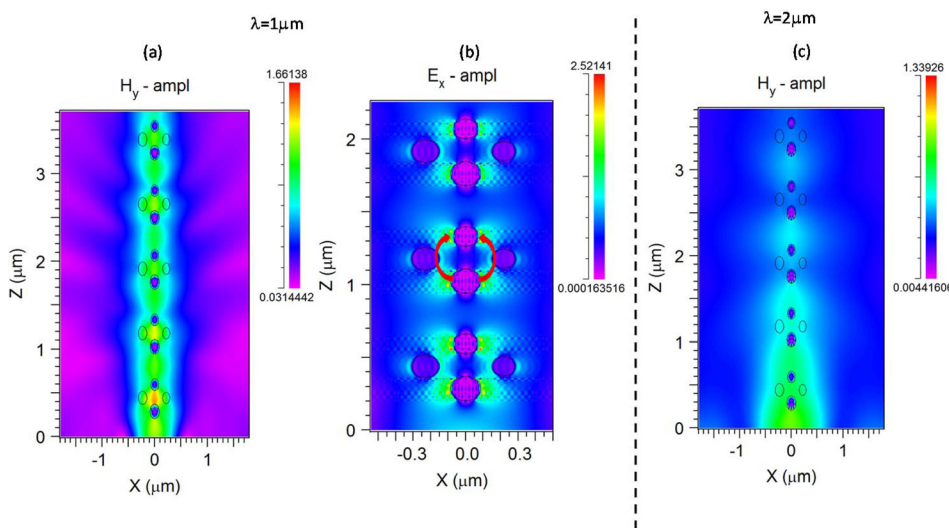


FIG. 8. The field profiles for the plasmonic NPWG with interlaced dielectric nano-particle (a)  $H_y$  field at design wavelength  $\lambda = 1\ \mu\text{m}$  (b)  $E_x$  field at design wavelength  $\lambda = 1\ \mu\text{m}$  (c)  $H_y$  field below cutoff  $\lambda = 2\ \mu\text{m}$ .

TABLE I. Comparison of attenuation factors and group velocities for different NPWG.

Light trapping structure	Plasmonic baseline	Dielectric baseline	Plasmonic core-shell	Dielectric core-shell
$v_g$ (m/s)	0.51c	0.44c	0.52c	0.49c
Attenuation factor, $\alpha$ (db/ $\mu\text{m}$ )	0.95	0.45	0.24	0.21
Light trapping structure	Plasmonic-Dielectric Hybrid	Dielectric supercell		
$v_g$ (m/s)	0.47c	0.44c		
Attenuation factor, $\alpha$ (db/ $\mu\text{m}$ )	0.25	0.05		

the field profile for  $\lambda = 0.5 \mu\text{m}$  in Fig. 6 in Sec. V where the propagation of the electromagnetic power decreases significantly along the NP chain. The significant attenuation at higher order modes for NPWG is due to the fact that the

waveguiding in NPWG is by successive Mie mode coupling. This is drastically different from conventional dielectric or metal slab waveguides where higher order modes can also propagate with attenuation not very different from

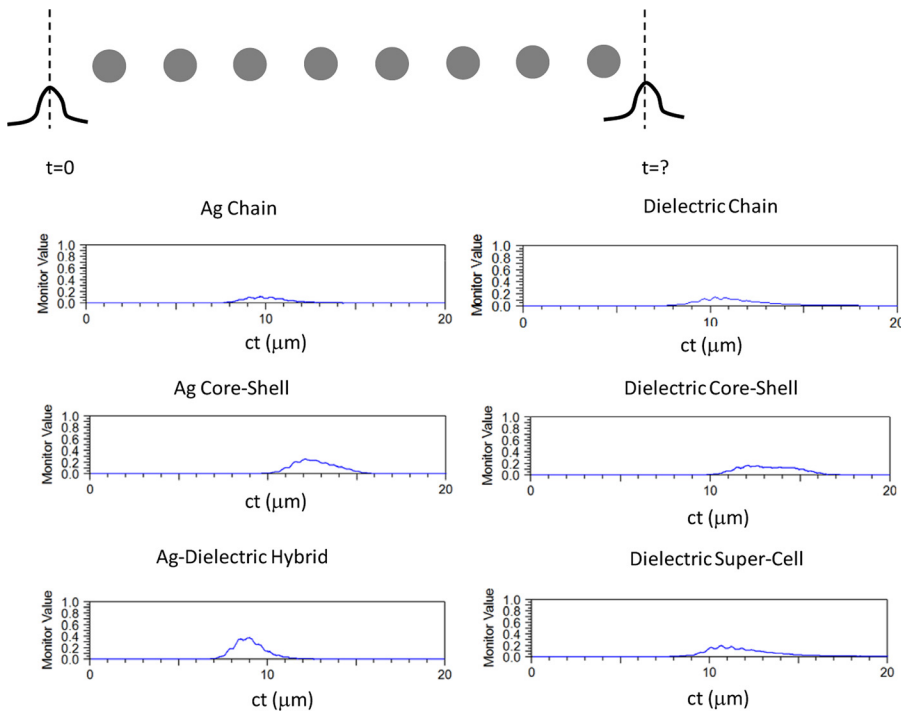


FIG. 9. The pulsed excitation for various NPWG structures in this study. Group velocity ( $v_g$ ) can be extracted from the pulsed excitation study by knowing the total traveling time for the pulse and the distance traveled along the NP chain.

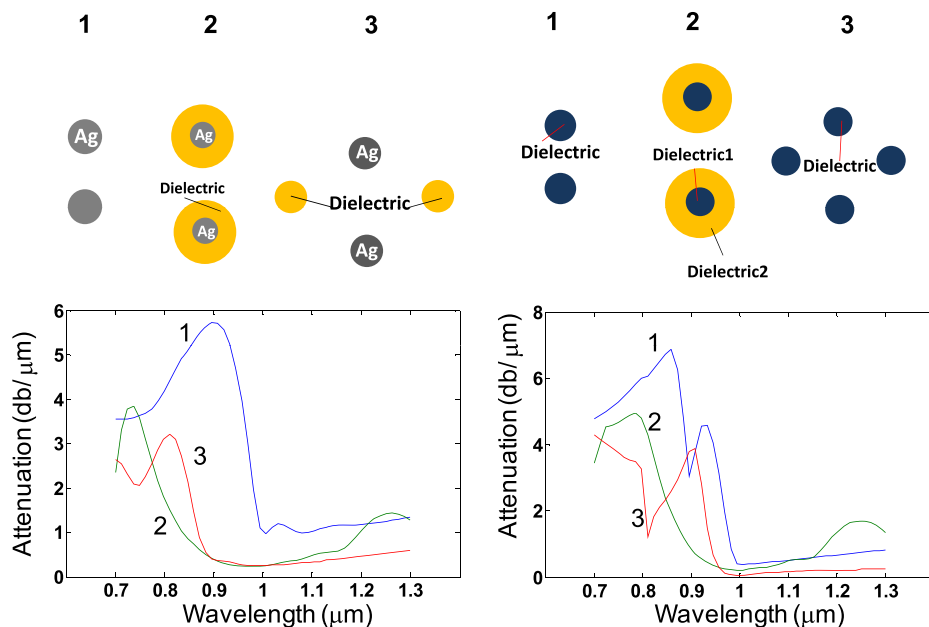


FIG. 10. The spectral responses for the various NPWG designs. (Left) plasmonic based designs. (Right) dielectric based designs.

fundamental modes. In order to operate at shorter wavelength, scaling of the optimized geometry can be conducted. Nevertheless, care should be taken that for plasmonic NPWG, the dielectric response of a metallic material can vary significantly over the spectrum, and the scaling of the geometry should be accompanied by re-selection of plasmonic materials. For excessive long wavelength, the guiding of NPs will gradually become inefficient. This is resulted from the fact that the wavelength is much larger than the NP diameters, and thus the waveguiding is deteriorated.

## VIII. CONCLUSION

Versatile designs of different NPWG configurations are examined in this work. Specifically, the core-shelled design for plasmonic NPWG enhances the energy transfer by reducing the plasmonic absorption. On the other hand, the core-shelled design for dielectric NPWG enhances the forward diffraction and thus promotes the Mie coupling between the dielectric NPs. On the other hand, the enhanced energy transfer for supercells design is through adding additional energy transfer paths for NP chains. For the dielectric-mediated plasmonic NPWG, the interlaced dielectric NP increases the mode coupling and reduces the plasmonic absorption loss by hybrid plasmonic-dielectric Mie scattering. The attenuation factor after geometry optimization is 0.21 dB/ $\mu\text{m}$  for dielectric NPWG using core-shelled design, and 0.24 dB/ $\mu\text{m}$  for plasmonic NPWG using core-shelled design. On the other hand, the attenuation factor after geometry optimization is 0.05 dB/ $\mu\text{m}$  and 0.25 dB/ $\mu\text{m}$ , for supercelled dielectric NPWG and for dielectric-mediated plasmonic NPWG, respectively. Therefore, as a whole, the lowest attenuation factor achieved in this work is by using supercelled dielectric NPWG, and it is 20-fold reduction compared to the baseline plasmonic NPWG, 8-fold reduction compared to the baseline dielectric NPWG. Finally, it is found that while plasmonic NPs can generally initiate very strong field emission, a well-designed dielectric NPWG can be more efficient than plasmonic ones due to zero plasmonic absorption. In addition, it is also found that the geometrical constraints for high transmittance and high group velocity are actually very similar, and this results in the fact that geometry optimized for high energy transfer rate also leads to high group velocity.

## ACKNOWLEDGMENTS

This work was funded by Ministry of Science and Technology, Taiwan, under Grant No. NSC 102-2221-E-009-121.

- <sup>1</sup>C. W. Berry, N. Wang, M. R. Hashemi, M. Unlu, and M. Jarrahi, *Nat. Commun.* **4**, 1622 (2013).
- <sup>2</sup>A. Politano, *Philos. Mag.* **92**(6), 768–778 (2012).
- <sup>3</sup>Q. Bao and K. P. Loh, *ACS Nano* **6**(5), 3677–3694 (2012).
- <sup>4</sup>A. Politano and G. Chiarello, *Nanoscale* **5**, 8215–8220 (2013).
- <sup>5</sup>A. Politano, *Plasmonics* **7**(1), 131–136 (2012).
- <sup>6</sup>J. R. Lakowicz, *Plasmonics* **1**(1), 5–33 (2006).
- <sup>7</sup>S. A. Maier, P. G. Kik, H. A. Atwater, S. Meltzer, E. Harel, B. E. Koel, and A. A. G. Requicha, *Nature Mater.* **2**, 229–232 (2003).
- <sup>8</sup>S. A. Maier, P. G. Kik, and H. A. Atwater, *Phys. Rev. B* **67**(20), 205402–205405 (2003).
- <sup>9</sup>J. R. Krenn, *Nature Mater.* **2**, 210–211 (2003).
- <sup>10</sup>A. Lin, S.-M. Fu, Y.-K. Chung, S.-y. Lai, and C.-W. Tseng, *Opt. Express* **21**(S1), A131–A145 (2013).
- <sup>11</sup>J. Du, S. Liu, Z. Lin, J. Zi, and S. T. Chui, *Phys. Rev. A* **83**, 035803 (2011).
- <sup>12</sup>K. Q. Le, A. Abass, B. Maes, P. Bienstman, and A. Alù, *Opt. Express* **20**(S1), A39–A50 (2012).
- <sup>13</sup>S. A. Mann, R. R. Grote, J. Richard, M. Osgood, and J. A. Schuller, *Opt. Express* **19**(25), 25729–25740 (2011).
- <sup>14</sup>Y. A. Akimov, W. S. Koh, S. Y. Sian, and S. Ren, *Appl. Phys. Lett.* **96**(7), 073111 (2010).
- <sup>15</sup>J. D. Joannopoulos, S. G. Johnson, R. D. Meade, and J. N. Winn, *Photonic Crystal: Molding the Flow of Light*, 2 ed. (Princeton University Press, Princeton, NJ, 2008).
- <sup>16</sup>J. Ma, L. J. Martínez, S. Fan, and M. L. Povinelli, *Opt. Express* **21**(2), 2463–2473 (2013).
- <sup>17</sup>S. Preblea, M. Lipson, and H. Lipson, *Appl. Phys. Lett.* **86**, 061111–061113 (2005).
- <sup>18</sup>B. Deken, S. Pekarek, and F. Dogan, *Comput. Mater. Sci.* **37**, 401–409 (2006).
- <sup>19</sup>H. Lipson and J. B. Pollack, *Nature* **406**, 974–978 (2000).
- <sup>20</sup>L. Shen, Z. Ye, and S. He, *Phys. Rev. B* **68**, 035101–035109 (2003).
- <sup>21</sup>Rsoft, *Rsoft CAD User Manual*, 8.2 ed. (Rsoft Design Group, New York, 2010).
- <sup>22</sup>H. A. Atwater and A. Polman, *Nature Mater.* **9**, 205–213 (2010).
- <sup>23</sup>A. C. Jones, R. L. Olmon, S. E. Skrabalak, B. J. Wiley, Y. N. Xia, and M. B. Raschke, *Nano Lett.* **9**(7), 2553–2558 (2009).
- <sup>24</sup>T. R. Jensen, M. D. Malinsky, C. L. Haynes, and R. P. V. Duyne, *J. Phys. Chem. B* **104**, 10549–10556 (2000).
- <sup>25</sup>B. Shen, Y. Huang, X. Duan, X. Ren, X. Zhang, and Q. Wang, *IEEE Photon. J.* **5**(2), 4500309 (2013).
- <sup>26</sup>S. L. Chuang, *Physics of Photonic Devices (Wiley Series in Pure and Applied Optics)*, 2 ed. (Wiley, New York, 2009).
- <sup>27</sup>P. Bhattacharya, *Semiconductor Optoelectronic Devices*, 2nd ed. (Prentice-Hall, Upper Saddle River, NJ, 2006).
- <sup>28</sup>D. K. Cheng, *Field and Wave Electromagnetics*, 2nd ed. (Addison-Wesley, Boston, MA, USA, 1989).